

Single-Channel Hadamard Encoded Endoscope for High-Frequency IVUS Imaging

Eric Simpson
Biomedical Engineering
Dalhousie University
Halifax, NS, Canada
eric.simpson@dal.ca

Katherine Latham
Biomedical Engineering
Dalhousie University
Halifax, NS, Canada
kate.latham@dal.ca

Christopher Samson
Biomedical Engineering
Dalhousie University
Halifax, NS, Canada
samsonchris.cs@gmail.com

J.K. Woodacre
Biomedical Engineering
Dalhousie University
Halifax, NS, Canada
jwoodacr@dal.ca

Tegan Aguiaga
Chemical Engineering
University of New Brunswick
Fredericton, NB, Canada
tegan.aguiaga@unb.ca

Jeremy A. Brown
Biomedical Engineering, Electrical and
Computer Engineering
Dalhousie University
Halifax, NS, Canada
j.brown@dal.ca

Abstract—A new image acquisition scheme is presented that is optimized for applications that require channel-limited transducers such as IVUS. During image acquisition, both the transmit and receive apertures are dynamically phase-encoded with a set of orthogonal (Hadamard) codes. The transducer's excitation and data collection are handled on a single RF channel. Simulations using the Field II software package showed an 18 dB improvement in SNR when compared to a synthetic aperture technique which multiplexes elements into a single RF channel. A 30 MHz transducer with an endoscopic form-factor was fabricated and used to demonstrate data collection and image reconstruction based on this Hadamard-encoding scheme. Experimentally-reconstructed images of a wire-target showed 50 dB of dynamic range.

Keywords—IVUS, Ultrasound transducers, High-frequency ultrasound imaging, Coded excitation, Hadamard encoding, Beamforming

I. INTRODUCTION

Certain high-frequency ultrasound imaging applications require that the transducer be packaged in a physically compact housing. For example, in intravascular ultrasound (IVUS) imaging, the transducer is housed in a miniaturized catheter ranging in size from 3.5 to 6 F (roughly 1.2 to 2 mm in diameter). This places significant limitations on the number of coaxial cables that can be run from the array elements to external systems compared to conventional linear or linear phased array (PA) transducers, which typically have between 64 and 256 channels. Because of space limitations, IVUS transducers have conventionally been limited to single-element transducers with the inherent trade-offs between depth-of-field and beamwidth. Synthetic aperture (SA) imaging is a common technique that allows for a significant reduction in system channels, while providing comparable image quality to traditional methods of image acquisition [1]. The reduction in channels results from multiplexing element signals through a small number of coax cables. Despite generating a two-way focus everywhere in the field, the low energy pulses resulting from the sparseness of the transmit aperture leads to poor SNR and depth of penetration.

In general, the signal-to-noise ratio (SNR) of a system can be expressed in dB as

$$SNR = 20 \log \left(\frac{A}{\sigma} \right), \quad (1)$$

where A is the amplitude of the received signal, and σ is the standard deviation of the noise signal.

Under the assumption that the noise present in an US imaging system is due to uncorrelated, electronic noise with constant variance [1], the expression for SNR for imaging systems employing conventional beamforming can be found in the following way: Since conventional N -element PA systems transmit on all elements, the amplitude of the reflected signal is scaled by a factor of N . Upon receive, the reflected signal is detected on all N elements and delayed and summed by the receive beamformer. The final result of both transmit and receive beamforming is that the amplitude of the received signal is increased by a factor of N^2 . Also, on receive, the noise is detected and incoherently summed on all N elements, and therefore the system noise is equal to $\sqrt{N\sigma^2}$. In order to compare the SNRs of various acquisition schemes, we can assume that the transmitted acoustic signal has unity amplitude and that the uncorrelated noise signals have a constant standard deviation $\sigma=1$. Using (1), the SNR of a conventional PA imaging scheme becomes

$$SNR = 20 \log \left(\frac{N^2}{\sqrt{N}} \right), \quad (2)$$

For the extreme case where only a single RF channel is available for image reconstruction, a synthetic aperture acquisition scheme would consist of multiplexing individual array elements and generating channel data in the following way: First, element 1 is repeatedly pulsed N times while receiving with each element sequentially until all N elements have received echoes from element 1. Next, element 2 is activated for transmitting N pulses, and each element is individually selected for receive. The process continues until all elements have been used for transmitting, resulting in a total of N^2 transmit events to generate a full channel data set for beamforming. Since the noise level sums incoherently for N^2 pulses, the SNR of this type of acquisition scheme is equal

to $20 \log(N)$, which is a \sqrt{N} reduction in SNR compared to the conventional PA case.

Previous work has demonstrated that orthogonal Hadamard codes can be applied to a fully activated transmit aperture in order to increase SNR over conventional SA imaging in one dimension [2-4]. The work presented here expands on this method by activating a set of independent orthogonal Hadamard codes on both the transmit and receive apertures. Since the transmit and receive apertures are coded independently, a full set of RF channel data equivalent to SA is obtained, using only a single RF transmit and receive channel. The advantage is that with this technique, the \sqrt{N} SNR improvement over SA is obtained while still utilizing only one RF channel. This technique has the potential to greatly increase the quality of IVUS imaging by moving to array based transducers. Since the technique only requires one RF channel, it is not limited by the small size of the IVUS catheters.

II. THEORY

Phase-encoding of transmissions has been previously shown as an effective way of increasing the SNR of an image. For example in [3], a set of N linear array elements was transmit encoded with a pattern of $+90$ or -90 degree phase shifts across the entire aperture, and demonstrated an M -times improvement in SNR, where M is the number of transmit events. If the patterns applied across the transmit elements are represented as row vectors containing $+1$ or -1 (corresponding to $+90$ or -90 degree phase shifts), a set of N , pair-wise orthogonal codes of length N forms an $[N \times N]$ Hadamard matrix. Hadamard matrices (H) have the property that

$$H^{-1} = \frac{1}{N} H^T. \quad (3)$$

For a set of N transmissions into the imaging field that are each encoded with unique Hadamard codes, let the matrix R represent the reflected signals received back at the array elements. That is,

$$R = \begin{bmatrix} r_{1,1}(t) & \cdots & r_{1,N}(t) \\ \vdots & \ddots & \vdots \\ r_{N,1}(t) & \cdots & r_{N,N}(t) \end{bmatrix}, \quad (4)$$

where $r_{i,j}(t)$ is the time-domain received signal, recorded on the i^{th} linear electrode for the j^{th} transmit event. R is related to the set of N encoded transmission by the matrix equation

$$R = HT\Phi, \quad (5)$$

where T is the $[N \times 1]$ transmit pulse matrix, H is the $[N \times N]$ Hadamard encoding matrix, and Φ is the two-way field transfer function.

Using the inverse property of (3), the decoded channel data can be found as

$$R' = H^T R = NIT\Phi = \begin{bmatrix} r'_{1,1}(t) & \cdots & r'_{1,N}(t) \\ \vdots & \ddots & \vdots \\ r'_{N,1}(t) & \cdots & r'_{N,N}(t) \end{bmatrix}, \quad (6)$$

where $r'_{i,j}(t)$ is the decoded time-domain received signal. Effectively, $r'_{i,j}(t)$ is the received signal on the i^{th} element

from transmitting with the j^{th} element. Note that for this previously demonstrated scheme, the aperture is not encoded on receive and channel data is received in parallel [3-5].

In the presented work, Hadamard encoding/decoding was implemented using a single RF channel by encoding the both the transmit aperture and switching to an independently encoded receive aperture. Encoding of transmit and receive apertures can be achieved by dicing a set of array electrodes on one side of an electrostrictive ceramic. When a bias voltage is applied to a region of an electrostrictor, the phase of the transmitted pulse is quantized to either $+90^\circ$ or -90° , depending on whether the bias is positive or negative. By applying a biasing pattern to the linear electrodes, the imaging aperture can be encoded for both transmit and receive. This can be done in real-time by dynamically changing the bias patterns during image acquisition. If the opposite side of the ceramic is a continuous planar electrode, the reflected signals received on the scratch-diced electrodes are superimposed and summed on a single system channel. This scheme is shown for both transmit and receive configurations in Fig. 1 (a) and (b).

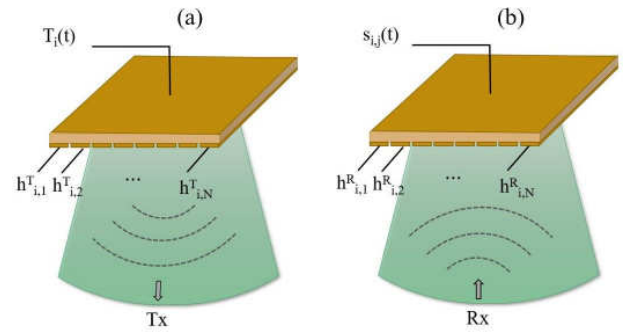


Fig. 1 Single RF channel transducer in (a) transmit mode, and (b) receive mode. In transmit mode, the scratch-diced electrodes have a bias pattern applied to them and the rf channels is used for pulsing. For receive, the bias pattern is switched, and the received signals are recorded on the elements, and superimposed on the single RF channel.

To understand how this acquisition scheme works, we adopt the following notation: Let $h_{i,j}^R$ be the j^{th} element coefficient, of the i^{th} receive aperture Hadamard code. Let $s_{i,j}(t)$ be the time-domain signal recorded on the single RF line resulting from transmitting with the i^{th} transmit aperture, and receiving with the j^{th} receive aperture.

For the case in which we both transmit and receive using the first Hadamard code, then the superimposed signal on the RF line, (namely $s_{1,1}$), would be

$$s_{1,1} = \sum_{i=1}^N r_{1,i} h_{1,i}^R \quad (7)$$

$$= [r_{1,1} \quad \cdots \quad r_{1,N}] \begin{bmatrix} h_{1,1}^R \\ \vdots \\ h_{1,N}^R \end{bmatrix}. \quad (8)$$

By keeping the transmit aperture fixed with Hadamard code 1, and cycling through all N receive aperture codes, we can construct a row vector (R_{TX1}), which consists of the all RF line signals for transmit Hadamard code 1.

$$R_{TX1} \equiv [s_{1,1} \quad \cdots \quad s_{1,N}] \quad (9)$$

$$= [\sum_{i=1}^N r_{1,i} h_{1,i}^R \quad \cdots \quad \sum_{i=1}^N r_{1,i} h_{1,N}^R] \quad (10)$$

$$= [r_{1,1} \quad \dots \quad r_{1,N}] \begin{bmatrix} h_{1,1}^R & \dots & h_{N,1}^R \\ \vdots & \ddots & \vdots \\ h_{1,N}^R & \dots & h_{N,N}^R \end{bmatrix} \quad (11)$$

Therefore, with the transmit aperture held constant with Hadamard code 1, if we cycle through all N receive apertures, we can uniquely solve for the first row of the encoded channel data matrix, R as

$$[r_{1,1} \quad \dots \quad r_{1,N}] = R_{TX1} \cdot H \quad (12)$$

Likewise, repeating this same process using transmit Hadamard code 2, we can solve for the 2nd row of R . After using all N transmit apertures we can individually construct each row of the matrix R , which can then be decoded into a complete set of channel data by (6).

The theoretical SNR of this acquisition scheme is $20 \log(N^{3/2})$, which provides a \sqrt{N} improvement in SNR compared to the SA scheme previously described, which utilizes a single RF channel.

III. SIMULATIONS

Simulations of the new imaging technique were carried out using the Field II software package [6], which uses a spatial impulse response method for modelling the behavior of acoustic transducers. The transducer was modeled to have a center frequency of 30 MHz, and included 64 linear electrodes, with a pitch of 54 μm , and extending 3 mm in the elevation direction. To simulate the affect of encoding the apertures on transmit and receive, the linear elements were ‘apodized’ using +1’s and -1’s, in accordance with the orthogonal rows of the 64x64 Hadamard matrix. To account for transducer only having a single RF channel, the resulting encoded receive signals recorded on the linear elements were summed. This simulates the affect of having a continuous planar electrode on one side of the ceramic, which is used as the only receive channel.

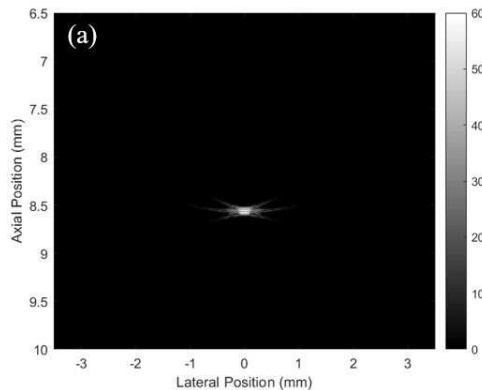


Fig. 2 Field II simulated point-spread and radiation pattern of a 64-element, 30 MHz phased-array. The data was simulated by Hadamard-encoding 64x64 transmit-receive events, and the channel image data was decoded and reconstructed offline.

Figs. 2 (a) and (b) show the point spread function and radiation pattern of the simulated single-channel Hadamard-encoded array. The point spread function is displayed with 60 dB of dynamic range.

To characterize the noise performance of this imaging technique, noise signals were included in the Field II model. Equal levels of AWGN were imposed onto the channel signals prior to decoding and beamforming for both the single-

channel Hadamard and synthetic aperture schemes. The resulting two-way radiation patterns are shown in Fig.3. The radiation patterns are normalized to the peak signal in the field for each acquisition scheme.

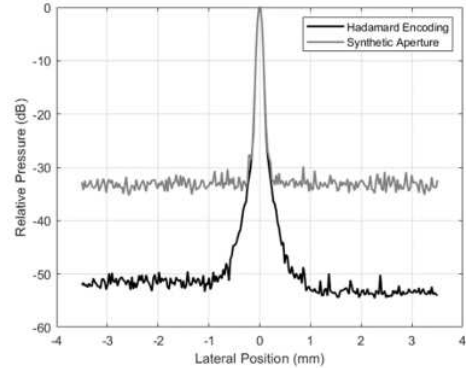
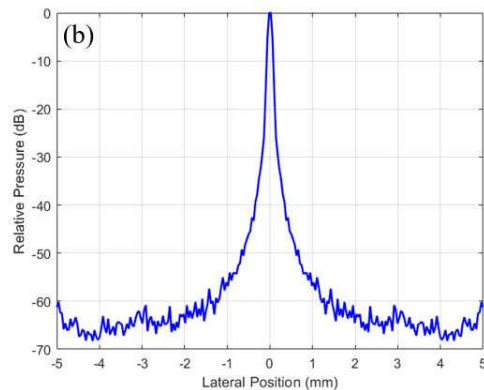


Fig. 3 Simulated radiation patterns for the Hadamard-encoding scheme and a single-element SA scheme. A fixed level of AWGN was added to the simulated receive signals prior to beamforming and image reconstruction.

It can be seen in the figure that once the affect noise included in the simulations, the side pedestal level for the SA scheme is roughly 18 dB (\sqrt{N}) higher than the Hadamard-encoding scheme.

IV. EXPERIMENTAL RESULTS

The single-channel Hadamard imaging technique was verified experimentally using a custom 30 MHz crossed-electrode array, which was previously developed by our group for high-frequency 3D imaging [7]. The array was fabricated on an electrostrictive ceramic substrate (PMN38, TRS technologies, Penn State, PA), and consists of 64x64 crossed linear electrodes, with a pitch of 54 μm , and extending 3.5 mm in the elevation direction. A compact endoscopic form factor is achieved using a wire bonding technique developed by Bezanson et al. in [8]. In this technique, a pair of long, flexible



PCBs are mounted flush with the elevation edges of the array stack with exposed cross-sectional pads that provide a bonding site for easy connectivity to the array elements via wire bonding. For a more detailed description of the fabrication technique, see [7,8].

For the purposes of demonstrating the single-channel Hadamard encoding scheme, 64 linear electrodes of the 128 element crossed-electrode array were used to reconstruct

images of a 25 μm thick wire target in a de-ionized water bath. To operate the array as single channel transducer, signals on the 64 linear elements were summed together and superimposed onto a single RF channel. The 64 linear electrodes on the opposite side of the ceramic were connected via the flex circuits the biasing circuitry required to encode the transmit and receive apertures.

Image data were collected using a 64-channel beamformer which was built in-house and includes a custom circuit for dynamically changing the transmit and receive biasing pattern. The system was configured to collect data from 64 orthogonally-encoded transmit apertures per frame, at a PRF of 10 kHz. To generate a complete set of channel

apertures through a set of 64 external system channels, dynamic aperture biasing can easily be provided through a simple digital ASIC integrated into the probe. In this case, the number of cables required to bias the apertures would be limited to a clock signal to control the dynamic bias switching, and two DC voltage lines to power the biasing ASIC.

The image data in this study was collected and reconstructed offline, however, the single-channel Hadamard encoding scheme could be easily adapted to generate images in real-time. For example, using a PRF of 40 kHz, the 64x64 transmit/receive events required for image reconstruction could theoretically be achieved at a frame-rate of 10 Hz.

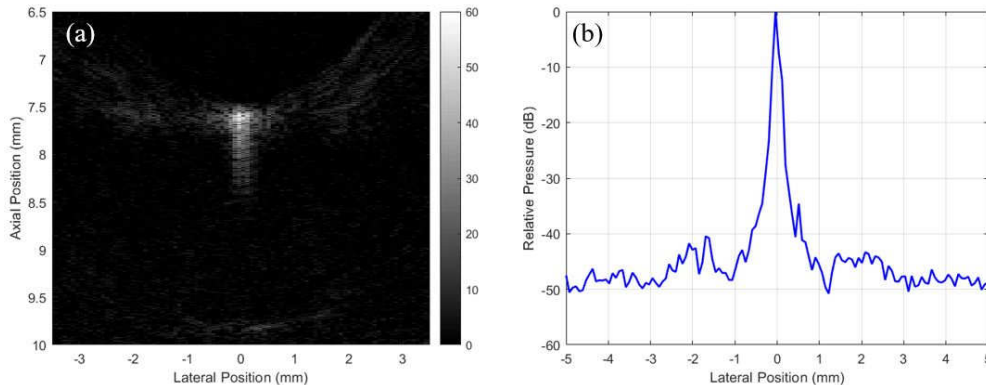


Fig. 4 Experimentally-measured point-spread and radiation pattern of using 64 elements of a 128-element, 30 MHz crossed-electrode array, The data was collected using Hadamard-encoding of 64x64 transmit-receive events.

data set for offline beamforming, it is required to collect signals for a set of 64 uniquely-encoded receive apertures for each of the 64 transmit codes. Once the 64 x 64 encoded transmit-receive events are complete, the data was decoded and beamformed offline to generate images that are focused everywhere in the field.

The experimentally reconstructed image and resulting point-spread function of the wire target are shown in Fig.4 (a) and (b) respectively. The images are displayed with 60 dB of dynamic range.

V. RESULTS/DISCUSSION

This work demonstrates the reconstruction of fully beamformed images using a 30 MHz transducer, which was configured to transmit and receive on a single RF channel. The new Hadamard encoding/decoding scheme allows for a theoretical \sqrt{N} SNR improvement over SA. Although the initial experimental results are promising, work is currently underway to fabricate a transducer optimized specifically for this method of image acquisition. For example, further improvements can be made in the transducer's elevation design. Although the experimentally-measured point spread function of a wire target shows a side-pedestal level of -50 dB with respect to the main peak, this can be greatly improved by including an elevation lens in the transducer design.

A transducer that is designed specifically for this imaging scheme can also be designed to minimize the number of external system channels required. Although the transducer used in this study provided biasing of transmit and receive

REFERENCES

- [1] M. Karaman, Pai-Chi Li and M. O'Donnell, "Synthetic aperture imaging for small scale systems," in *IEEE Transactions on Ultrasonics, Ferroelectrics, and Frequency Control*, vol. 42, no. 3, pp. 429-442, May 1995.
- [2] T. Harrison, A. Sampaleanu and R. J. Zemp, "S-sequence spatially-encoded synthetic aperture ultrasound imaging [Correspondence]," in *IEEE Transactions on Ultrasonics, Ferroelectrics, and Frequency Control*, vol. 61, no. 5, pp. 886-890, May 2014.
- [3] R. Y. Chiao, L. J. Thomas and S. D. Silverstein, "Sparse array imaging with spatially-encoded transmits," *1997 IEEE Ultrasonics Symposium Proceedings. An International Symposium (Cat. No.97CH36118)*, Toronto, Ont., Canada, 1997, pp. 1679-1682 vol.2.
- [4] C. Samson, E. Simpson, R. Adamson and J. A. Brown, "Sparse Orthogonal Diverging Wave Imaging on a High-Frequency Phased Array," *2018 IEEE International Ultrasonics Symposium (IUS)*, Kobe, 2018, pp. 1-4.
- [5] C. Ceroici, K. Latham, B. A. Greenlay, J. A. Brown and R. J. Zemp, "Fast Orthogonal Row-Column Electronic Scanning Experiments and Comparisons," in *IEEE Transactions on Ultrasonics, Ferroelectrics, and Frequency Control*, vol. 66, no. 6, pp. 1093-1101, June 2019.
- [6] J. Jensen, "Field: a program for simulating ultrasound systems," *Medical & Biological Engineering & Computing*, vol. 34, no. Supplement 1, Part 1, pp. 351-353, 1996.
- [7] K. Latham, C. Ceroici, C. A. Samson, R. J. Zemp and J. A. Brown, "Simultaneous Azimuth and Fresnel Elevation Compounding: A Fast 3-D Imaging Technique for Crossed-Electrode Arrays," in *IEEE Transactions on Ultrasonics, Ferroelectrics, and Frequency Control*, vol. 65, no. 9, pp. 1657-1668, Sept. 2018.
- [8] A. Bezanson, R. Adamson and J. A. Brown, "Fabrication and performance of a miniaturized 64-element high-frequency endoscopic phased array," in *IEEE Transactions on Ultrasonics, Ferroelectrics, and Frequency Control*, vol. 61, no. 1, pp. 33-43, January 2014.